 doi 10.12122/j.issn.1673-4254.2025.11.07 J South Med Univ, 2025, 45(11): 2350-2357

Tau蛋白沉积与脑代谢物的关联性：N-乙酰天门冬氨酸与肌酸作为进展期阿尔茨海默病的潜在生物标志物

李孝媛[1]，张逸悦[1]，顾雨铖[1]，陈霓红[2]，钱鑫宇[1]，张朋俊[1]，郝佳欣[3]，王 峰[1]
南京医科大学附属南京医院[1]核医学科，[2]神经内科，江苏 南京 210000；[3]上海联影医疗科技股份有限公司，上海 201807

摘要：目的 通过精确的空间映射，探索阿尔茨海默病（AD）患者Tau蛋白与氢质子磁共振波谱（^{1}H-MRS）所检测的脑内生化代谢物间的潜在关联。**方法** 收集2022年4月~2024年12月南京市第一医院核医学科共64例AD Tau^{+}患者（PT组）和29例健康志愿者（HC组）的^{18}F-APN-1607 PET/MR脑显像及同步采集的多体素^{1}H-MRS数据，对PET/MR数据进行视觉分析和基于体素的分析，以研究AD患者Tau蛋白沉积模式。在^{1}H-MRS扫描视野内筛选有效体素，并记录各有效体素内的PET标准摄取值比率（SUVr）以及各代谢物水平（含代谢物比值）：N-乙酰天门冬氨酸（NAA）、胆碱（Cho）、肌酸（Cr）、NAA/Cr、Cho/Cr。通过对Tau PET视觉分析，将PT组内各有效体素分为Tau阳性体素（Tau^{+}体素）和Tau阴性体素（Tau^{-}体素）。比较各组间PET和^{1}H-MRS指标的差异，并分析Tau^{+}体素内代谢物水平（含代谢物比值）与Tau PET SUVr之间的相关性。**结果** 在双侧额叶（30.07%）、顶叶（29.96%）、颞叶（21.07%）、枕叶（15.89%），PT组相较于HC组存在显著的Tau蛋白沉积。^{1}H-MRS扫描视野内共纳入有效体素2236个，PT组体素1422个（其中Tau^{+}体素994个、Tau^{-}体素428个），HC组体素814个。相较于HC组，PT组的NAA水平降低、SUVr增高（P<0.05）。亚组分析结果显示，与Tau^{-}体素相比，Tau^{+}体素的SUVr增高、Cr和Cho/Cr降低（P<0.05）；与HC组相比，Tau^{+}体素的SUVr增高、Cr降低（P<0.05）；与HC组相比，Tau^{-}体素的NAA降低（P=0.004）。Cho和NAA/Cr在各亚组间的差异无统计学意义（P>0.05）。Tau^{+}体素内NAA、Cho、Cr与SUVr呈负相关（P<0.001）。**结论** 进展期AD患者脑内Tau蛋白沉积显著且和部分代谢物水平改变相关。NAA水平的降低在Tau蛋白沉积前期及早期阶段更明显，Cr水平的改变在Tau蛋白沉积区域更显著，提示NAA及Cr可以为AD患者脑内Tau蛋白沉积的潜在生物标志物，为AD的早期诊断和疗效评估提供依据。

关键词：阿尔茨海默病；正电子发射断层扫描/磁共振成像；Tau蛋白；^{18}F-APN-1607；N-乙酰天门冬氨酸

Association between Tau protein deposition and brain metabolites: N-acetylaspartate and creatine as potential biomarkers for advanced Alzheimer's disease

LI Xiaoyuan[1], ZHANG Yiyue[1], GU Yucheng[1], CHEN Nihong[2], QIAN Xinyu[1], ZHANG Pengjun[1], HAO Jiaxin[3], WANG Feng[1]
[1]Department of Nuclear Medicine, [2]Department of Neurology, Nanjing First Hospital, Nanjing Medical University, Nanjing 210000, China; [3]Shanghai United Imaging Healthcare Co., Ltd., Shanghai 201807, China

Abstract: Objective To investigate the associations between Tau protein deposition and brain biochemical metabolites detected by proton magnetic resonance spectroscopy (^{1}H-MRS) in patients with advanced Alzheimer's disease (AD). **Methods** From April, 2022 to December, 2024, 64 Tau-positive AD patients and 29 healthy individuals underwent ^{18}F-APN-1607 PET/MR and simultaneously acquired multi-voxel ^{1}H-MRS in the Department of Nuclear Medicine, Nanjing First Hospital. Visual analysis and voxel-based analysis of PET/MR data were performed to investigate the Tau protein deposition patterns in AD patients. Valid voxels within the ^{1}H-MRS field of view were selected, and their standardized uptake value ratio (SUVr) in PET and metabolite levels of N-acetylaspartate (NAA), choline (Cho), creatine (Cr), NAA/Cr, and Cho/Cr were recorded. The Tau-positive (Tau^{+}) voxels and Tau-negative (Tau^{-}) voxels of the AD patients were compared for PET and ^{1}H-MRS parameters, and the correlations between the metabolites and Tau PET SUVr within Tau^{+} voxels were analyzed. **Results** Significant Tau protein deposition were observed in the AD patients, involving mainly the bilateral frontal lobes (30.07%), parietal lobes (29.96%), temporal lobes (21.07%), and occipital lobes (15.89%). A total of 1422 valid voxels in AD group (including 994 Tau^{+} and 428 Tau^{-} voxels) and 814 voxels in the control group were selected. The AD patients showed significantly decreased NAA level and increased SUVr compared with the control group (P<0.05). Subgroup analyses revealed that Tau^{+} voxels had higher SUVr and lower Cr and Cho/Cr than Tau^{-} voxels (P<0.05). Compared with the control group, Tau^{+} voxels exhibited higher SUVr and lower Cr (P<0.05), while Tau^{-} voxels showed lower NAA (P=0.004). No significant differences were found in Cho or NAA/Cr among the subgroups (P>0.05). Within Tau^{+} voxels, NAA, Cho, and Cr were negatively correlated with SUVr (P<0.001). **Conclusion** The patients with progressive AD have significant Tau protein deposition in the brain, which is correlated with alterations in metabolite levels. Decreased NAA is more prominent in early or pre-tau deposition stages, while Cr changes is more significant in the regions with Tau protein deposition, suggesting the potential of NAA and Cr as biomarkers for Tau protein deposition in AD for disease monitoring and treatment evaluation.

Keywords: Alzheimer's disease; positron emission tomography/magnetic resonance imaging; Tau protein; ^{18}F-APN-1607; N-acetylaspartate

收稿日期：2025-07-03
基金项目：国家重点研发计划（2022YFC2406900）；江苏省重点学科/实验室建设单位（JSDW202247）
作者简介：李孝媛，在读博士研究生，主治医师，E-mail: xiaoyuanlee0317@foxmail.com
通信作者：王 峰，博士生导师，E-mail: fengwangcn@hotmail.com

阿尔茨海默病(AD)是一种以认知功能障碍为特征的神经系统退行性疾病,其核心病理标志包括β淀粉样蛋白(Aβ)沉积和Tau蛋白异常磷酸化形成的神经原纤维缠结(NFTs)[1,2]。近年来,AT(N)生物标志物框架已成为AD诊断和分期的金标准[3,4],其中Tau蛋白(T)的时空分布特征不仅与疾病进展密切相关,更是神经变性(N)的直接驱动因素[5-7]。然而,Tau蛋白沉积如何通过局部代谢紊乱导致神经元功能障碍,仍是亟待解决的关键问题。

磁共振波谱(MRS)技术可无创检测脑内代谢物,如N-乙酰天门冬氨酸(NAA)、胆碱(Cho)、肌酸(Cr)的水平变化,进而反映神经元损伤和胶质细胞活化[8,9]。既往研究多通过分析脑脊液或血液Tau蛋白指标与特定脑区MRS参数的关联[10],但忽视了Tau病理的空间异质性,且不同脑区生化代谢响应存在差异。本研究拟通过^{18}F-APN-1607 PET/MR联合显像,整合高分辨率Tau-PET成像与多体素MRS技术,辅以结构MRI的精准解剖配准,建立体素水平Tau病理与代谢微环境的直接映射,精准分析AD患者脑内Tau蛋白负荷与MRS代谢物水平的点对点相关性,为AD的早期诊断和未来多靶点诊疗的疗效评估开发潜在影像学生物标记。

1 资料和方法

1.1 研究对象

连续纳入2022年4月~2024年12月在南京市第一医院核医学科接受^{18}F-APN-1607 PET/MR多模态脑显像检查的AD Tau$^+$患者(PT组),及与PT组年龄匹配的健康志愿者(HC组)。纳入标准:AD诊断采用2024年美国国家衰老研究所与阿尔茨海默病协会诊断标准[3];所有被试者均出现进行性认知下降,且接受临床神经心理学测试[简易智力状态检查量表(MMSE)评分≤26;蒙特利尔认知评估量表(MoCA)评分≤26];通过^{18}F-AV45 PET显像或脑脊液检查明确Aβ阳性。符合AD诊断且^{18}F-APN-1607 PET/MR视觉判断为阳性者纳入PT组;MMSE评分>26、MoCa评分>26且经^{18}F-AV45 PET显像证实脑内Aβ阴性者纳入HC组。排除标准:PET/MR检查禁忌;临床或影像学资料不全;伴有其他脑病变、脑血管疾病、创伤、精神疾病等。

最终共纳入93例研究对象,其中PT组64例(男性25例,女性39例),年龄50~88(68.48±8.98)岁;HC组29例(男性13例,女性16例),年龄50~76(61.53±9.81)岁;收集两组受试者性别、年龄、受教育年限、MMSE、MoCA、临床痴呆评定量表(CDR)评分及PET/MR脑部影像学资料。本研究经本院伦理委员会批准(伦理批号:YW20211224-08),所有受试者均签署知情同意书。

1.2 方法

1.2.1 图像采集 所有受试者经静脉注射^{18}F-APN-1607(370 MBq,放射性合成前体由苏州新旭医药有限公司提供)后安静休息90 min,随后使用PET/MR(上海联影医疗科技有限公司,uPMR790)行20 min PET三维扫描,并采用有序子集期望最大化算法进行图像重建。同步进行多参数MRI序列采集,磁共振场强为3.0T,使用24通道头颈联合线圈以提高信噪比。采集序列包括:3D-T1WI(重复时间7.2 ms,回波时间3 ms,翻转角10°,反转时间750 ms,体素1 mm×1 mm×1 mm)、^{1}H-MRS(重复时间1500 ms,回波时间144 ms,翻转角90°,视野256 mm×256 mm,体素1 mm×1 mm×1 mm)。^{1}H-MRS采集时,扫描视野需严格避开鼻窦、脑室等和脑组织信号差异较大的区域以确保匀场效果,局部匀场需达到水峰半高宽<15 Hz后方可采集,本研究^{1}H-MRS采集范围覆盖双侧额顶叶皮层区(图1)。

1.2.2 图像预处理 基于Matlab 2018b使用SPM12软件将PET图像配准到3D T1WI图像空间。随后利用非线性变换,将配准后的PET图像标准化至蒙特利尔神经病学研究所(MNI)标准空间,并用半高宽8 mm×8 mm×8 mm的高斯滤波对标准化后的图像进行空间平滑。以小脑皮质为参考区域[11],通过图像计算器计算全脑的标准摄取值比率(SUVr),获得预处理后的PET SUVr数据。

1.2.3 PET图像视觉分析 由2位具有5年以上神经影像经验的核医学科医生视觉分析两组受试者的^{18}F-APN-1607 PET/MR脑显像数据,总结AD患者Tau PET放射性示踪剂摄取分布特征。

1.2.4 PET图像基于体素的分析 采用SPM12软件进行基于体素的双样本t检验,比较PT组与HC组Tau蛋白沉积的空间分布差异。统计分析模型中纳入年龄、性别、受教育年限作为协变量以控制潜在混杂效应,以排除小脑的全脑模板为分析范围,采用多重比较的总体误差校正(FWE)方法校正,以FWE校正后P<0.05为差异有统计学意义,统计结果采用Xjview和BrainNet-Viewer软件呈现。

1.2.5 ^{1}H-MRS数据分析 采用SPM12的"New Segment"模块分割个体T1图像为灰质(GM)、白质(WM)和脑脊液(CSF)成分,得到灰质概率图,提取灰质概率≥0.4的体素,生成灰质模板。将^{1}H-MRS扫描视野映射到个体灰质模板上,通过视觉评估判断每个波谱体素的灰质占比是否超过2/3,灰质占比超过2/3的体素纳入后续统计分析。对于符合筛选标准的体素,逐体素记录以下代谢物水平及比值:Cr、NAA、Cho、NAA/Cr、Cho/Cr。此外,将^{1}H-MRS扫描视野映射到同层面PET/MR融合图像中(图1),记录各体素的标准摄取值(SUV),并以小脑皮层作为参考区域[11]计算各体素的SUVr。针对PT组体素,由2位具有5年以上神经影像经验的核医学科医生视觉评估各体素Tau PET摄取特征,评估结果一致时,将纳入评估的体素分为Tau$^+$体素和Tau$^-$体素,评估结果不一致的体素暂不纳入分组分析。

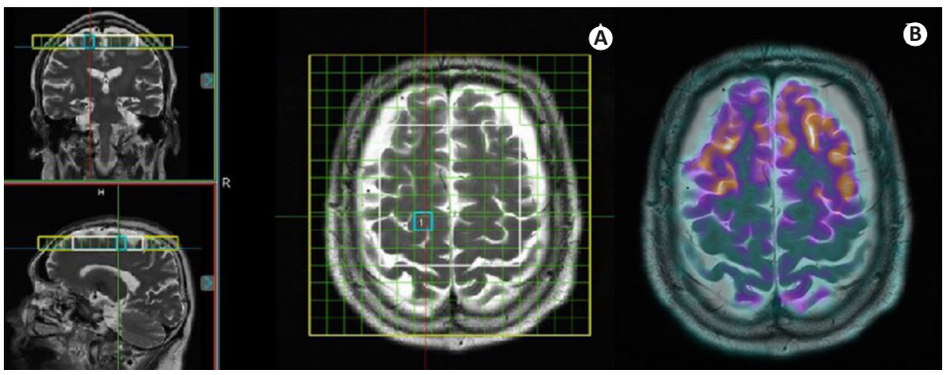

图1 1例AD患者的PET/MRS图像

Fig.1 PET/MRS imaging of a female AD patient (76 years old, education years: 0; MMSE: 0; MoCa: 0; CDR: 3). **A:** Coronal, sagittal, and axial localization images of MRS acquisition site, where the yellow box indicates the homogenization region, the white box denotes the MRS acquisition area, and the blue box outlines the selected voxel. **B:** Co-registered PET/MR fusion image at the same level as the MRS acquisition.

1.3 统计学分析

本研究采用SPSS26.0软件进行统计分析，计数资料以*n*(%)表示，组间比较采用卡方检验。符合正态分布的计量资料以均数±标准差表示，组间比较采用方差分析；当方差分析显示总体差异有统计学意义时，采用Bonferroni法进行组间两两比较。相关性分析使用皮尔逊相关分析（双尾检验），并通过Bonferroni法进行事后检验，相关系数记为*r*，以*P*<0.05为差异具有统计学意义。

2 结果

2.1 临床资料比较

PT组和HC组在性别、年龄、受教育年限的差异无统计学意义（*P*>0.05）。PT组的MMSE评分和MoCA评分低于HC组，CDR评分高于HC组（*P*<0.001，表1）。

表1 PT组和HC组临床资料比较

Tab.1 Comparison of clinical information of the AD patients (PT group) and the healthy control (HC) group (*Mean*±*SD*)

Variables	PT group (*n*=64)	HC group (*n*=29)	*P*
Gender (male/female, *n*)	25/39	13/16	0.767
Age (year)	68.48±8.98	61.53±9.81	0.382
Education years (year)	9.46±3.56	11.94±3.05	0.440
MMSE score (point)	19.45±7.55	28.59±1.45	<0.001
MoCA score (point)	15.63±7.61	26.66±2.83	<0.001
CDR score (point)	0.96±0.70	0.02±0.09	<0.001

MMSE: Mini-mental state examination; MoCA: Montreal cognitive assessment; CDR Clinical dementia rating.

2.2 PET视觉分析结果

^{18}F-APN-1607 PET/MR脑显像视觉分析结果显示，HC组仅双侧脉络丛区域可见生理性脱靶摄取，全脑皮层区未见明显放射性摄取；PT组除脉络丛生理性脱靶摄取外，双侧额、顶、颞叶皮层区可见弥漫分布的不均匀放射性摄取增高（图2）。

2.3 PET基于体素的分析结果

PT组和HC组预处理后PET SUVr数据的双样本*t*检验结果显示，PT组大脑皮层存在弥漫性Tau蛋白沉积，多个体素集群的SUVr值高于HC组（*P*<0.05，FWE校正，图3），无SUVr值降低的体素集群。与HC组相比，PT组Tau蛋白沉积增加区域主要分布在双侧额叶（30.07%）、顶叶（29.96%）、颞叶（21.07%）、枕叶（15.89%）。Tau蛋白沉积增加的峰值点MNI坐标为[27,-33,-18]，位于右侧梭状回。

2.4 体素内代谢物水平与Tau PET SUVr的组间比较及相关性分析

2.4.1 PT组与HC组的对比 ^{1}H-MRS的扫描视野内共采集5952个体素，筛选后获得有效体素2236个（PT组1422个、HC组814个）。与HC组相比，PT组的NAA水平减低、Tau PET SUVr增高，差异有统计学意义（*P*<0.05，表2），Cr、Cho、Cho/Cr、NAA/Cr的组间差异无统计学意义（*P*>0.05）。

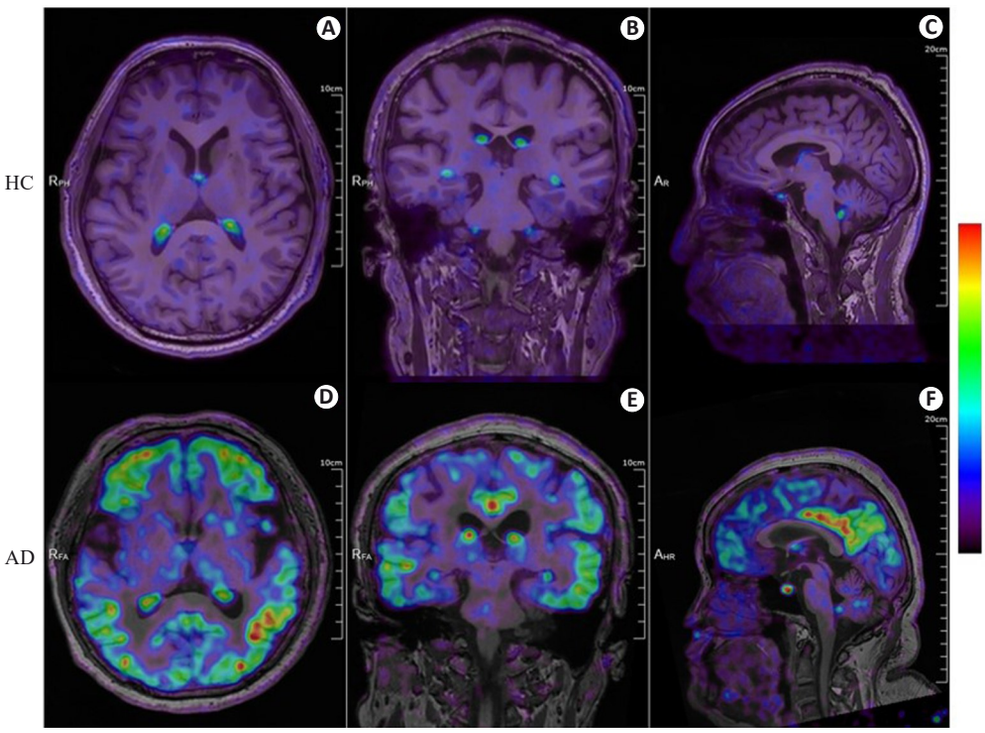

图2 1例HC和1例PT组AD患者的^{18}F-APN-1607 PET/MR融合图像

Fig.2 ^{18}F-APN-1607 PET/MR fusion imaging of a healthy control individual and an AD patient. **A-C:** Axial, coronal, and sagittal PET/MR fusion images of the brain of a male healthy control individual (72 years old, education years: 12; MMSE: 28, MoCa: 29; CDR: 0), showing physiological uptake in the choroid plexus without significant deposition of Tau protein in the remaining cerebrum and cerebellum. **D-F:** Axial, coronal, and sagittal PET/MR fusion images of the brain of a female AD patient (58 years old, education years: 12; MMSE: 5; MoCa: 2; CDR: 2) with diffuse and heterogeneous Tau protein deposition in the bilateral frontal, parietal, temporal, and occipital cortical regions. The color bar in the figure represents SUV.

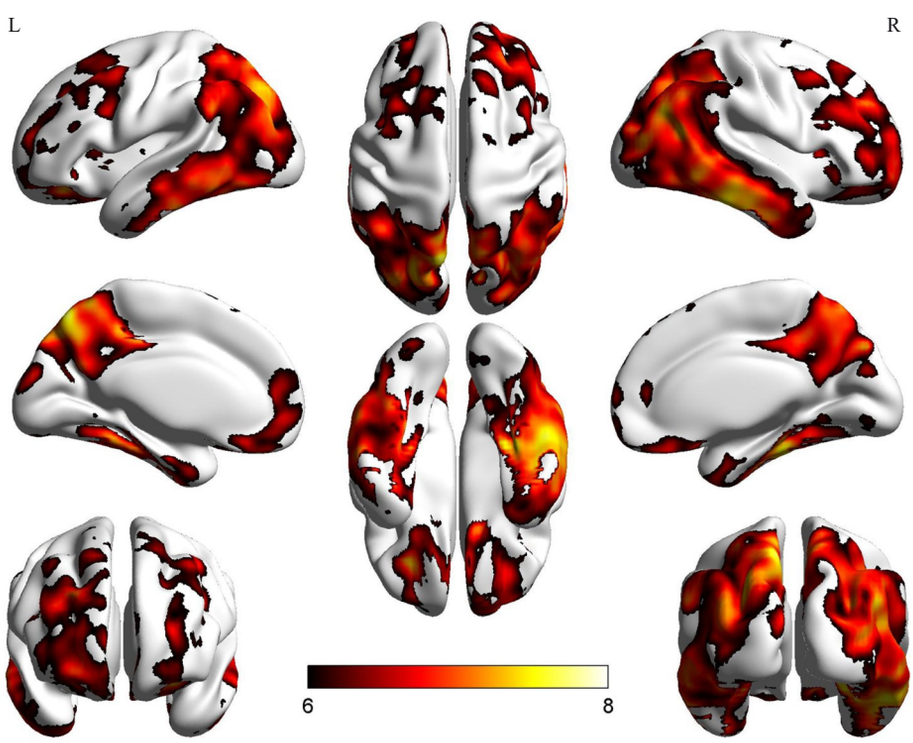

图3 基于体素的分析方法得到的PT组Tau蛋白沉积显著增加的区域

Fig.3 Regions of significantly increased Tau protein deposition in the PT group as determined by voxel-based analysis methods. The color bar in the figure represents the statistical t-values; L: Left cerebral hemisphere; R: Right cerebral hemisphere.

表2 PT组和HC组代谢物水平(含代谢物比值)和Tau PET SUVr组间比较结果

Tab. 2 Inter-group comparison of metabolite levels (or ratios) and Tau PET standardized uptake values between PT group and HC group (*Mean±SD*)

Variables	PT group	HC group	*P*
Voxel (*n*)	1422	814	-
Cr	29.02±12.07	28.97±10.71	0.063
Cho	24.58±11.16	24.47±11.40	0.829
NAA	45.02±20.54	47.03±18.84	0.022
Cho/Cr	0.856±0.239	0.864±0.219	0.406
NAA/Cr	1.660±0.663	1.742±0.564	0.065
SUVr	1.604±0.877	0.902±0.212	<0.001

Cr: Creatine; Cho: Choline; NAA: N-acetylaspartate; SUVr: Standardized uptake value ratio.

2.4.2 Tau^+体素、Tau^-体素与HC组体素亚组分析 PT组1422个有效体素分为Tau^+体素(994个,69.90%)和Tau^-体素组(428个,30.09%)。亚组分析结果显示:与Tau^-体素相比,Tau^+体素的SUVr增高(P<0.001),Cr和Cho/Cr降低(P<0.05);与HC组体素相比,Tau^+体素的SUVr增高(P<0.001),Cr减低(P=0.004),Tau^-体素的NAA降低(P=0.004)。Cho和NAA/Cr在3组间的差异无统计学意义(P>0.05,表3)。

表3 PT组体素亚分组后代谢物水平(含代谢物比值)和Tau PET SUVr组间比较结果

Tab.3 Inter-group comparison of metabolite levels (or ratios) and Tau PET SUVr following subgrouping of PT group voxels (*Mean±SD*)

Variables	Tau^+voxel	Tau^-voxel	HC voxel	*P*	P_1	P_2	P_3
Voxel (*n*)	994	428	814		-	-	-
Cr	27.11±11.92	29.84±12.05	28.97±10.71	<0.001	0.004	0.495	<0.001
Cho	24.90±10.92	23.82±11.66	24.47±11.40	0.242	-	-	-
NAA	45.82±20.17	43.17±21.28	47.03±18.84	0.005	0.596	0.004	0.065
Cho/Cr	0.844±0.246	0.882±0.209	0.864±0.219	0.014	0.212	0.592	0.015
NAA/Cr	1.676±1.380	1.622±0.588	1.742±0.564	0.119	-	-	-
SUVr	1.921±0.871	0.870±0.149	0.902±0.212	<0.001	<0.001	0.999	<0.001

P: Tau^+voxel *vs* Tau^-voxel *vs* HC; P_1: Tau^+voxel *vs* HC; P_2: Tau^-voxel *vs* HC; P_3: Tau+voxel *vs* Tau-voxel.

2.4.3 相关性分析 994个Tau^+体素各代谢物水平(含代谢物比值)与Tau PET SUVr的相关性分析结果显示,NAA、Cho、Cr与PET SUVr均呈负相关性(P<0.001,表4、图4);Cho/Cr、NAA/Cr与PET SUVr之间无相关性(P>0.05)。

表4 Tau^+体素组内各代谢物水平(含代谢物比值)和Tau PET SUVr的相关性分析结果

Tab. 4 Correlation analysis of metabolite levels (or ratios) and Tau PET SUVr in Tau^+ voxel

Variables	*r*	*P*
Cr	-0.161	<0.001
Cho	-0.176	<0.001
NAA	-0.200	<0.001
Cho/Cr	-0.058	0.787
NAA/Cr	-0.009	0.069

3 讨论

AD的AT(N)诊断框架通过β-淀粉样蛋白(A)、Tau蛋白(T)、神经变性(N)三大核心生物标志物的组合实现对AD各临床阶段的精准分期,为临床提供了标准化诊疗路径,是AD诊断模式转变为"生物标志物驱动"的关键进展[3,4]。Aβ沉积主要通过小胶质细胞激活产生神经毒性[12],而Tau蛋白沉积位于细胞内,与疾病进展关系更为密切,也是神经变性(N)的直接驱动因素[5-7]。本研究通过^{18}F-APN-1607 PET/MR多模态脑显像实现AD患者脑内病理性Tau蛋白沉积的空间可视化,同时将多体素波谱采集野三维定位映射到高分辨率Tau-PET,在体素水平建立Tau病理与^{1}H-MRS所检测代谢物水平的精准对应,分析AD患者脑内Tau蛋白沉积对代谢改变的影响。

本研究视觉分析和基于体素的分析均显示,AD组较HC组存在广泛大脑皮层Tau蛋白沉积,与既往研究

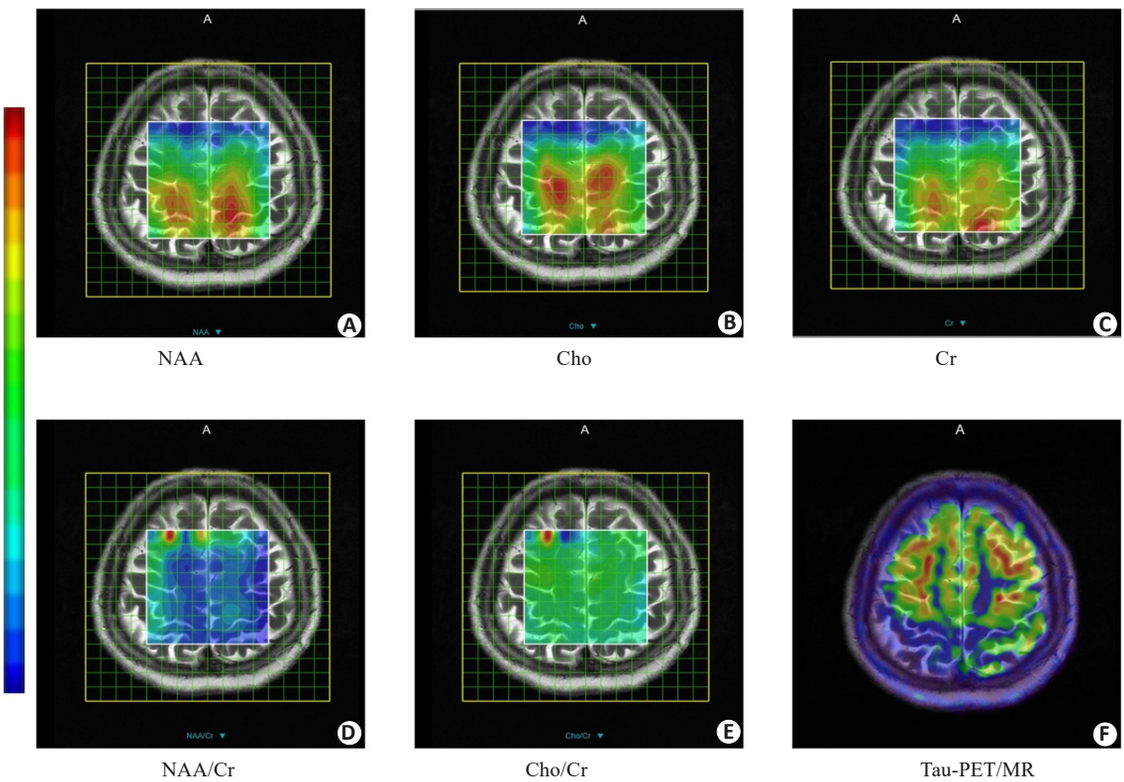

图4 1例PT组AD患者的^{1}H-MRS代谢物热图及^{18}F-APN-1607 PET/MR融合图像

Fig. 4 ^{1}H-MRS metabolite heatmap and ^{18}F-APN-1607 PET/MR fusion image of an AD patient. **A-E:** Heat maps of NAA, Cho, Cr, NAA/Cr, and Cho/Cr, respectively. **F:** ^{18}F-APN-1607 PET/MR fusion image of the AD patient (female, 58 years old, education years: 12; MMSE: 5; MoCa: 2; CDR: 2). NAA, Cho and Cr are lower in the Tau protein deposition area, while NAA/Cr and Cho/Cr showed no significant differences between the Tau protein deposition area and the non-Tau protein deposition area.

结果一致[13-17]。正常Tau蛋白为一种微管相关蛋白，过度磷酸化导致NFTs形成[2, 18, 19]。本研究结果显示，AD患者Tau蛋白沉积主要分布于额叶、顶叶（两者受累比例接近），其次为颞叶，枕叶受累比例最低，符合Braak分期描述的NFTs扩散模式[20-23]。基于体素的分析显示峰值坐标点位于右侧梭状回，该区域Tau蛋白沉积差异最显著，既往研究表明梭状回具有AD表观遗传特征[24]，以上均提示其在AD病理进程中可能具有重要作用。

^{1}H-MRS技术可无创检测患者脑内代谢物水平变化辅助疾病诊断与机制研究。既往研究表明，AD患者脑内NAA、Cho和Cr等代谢物水平的变化在疾病早期即已出现，且可在临床症状出现前被^{1}H-MRS检测到。NAA作为神经元完整性标志物，其浓度降低是神经元损伤的早期指征[25, 26]。本研究结果显示，PT组AD患者脑内NAA水平低于HC组，与既往研究报道的AD患者海马体、颞叶和顶叶等关键脑区NAA水平降低结果一致[25, 27, 28]。NAA水平的降低可能与Tau蛋白沉积、Aβ聚集以及神经炎症、氧化应激等多种病理机制相关[25-29]。本研究亚组分析结果显示，与HC组相比，NAA在Tau^{-}体素降低，而在Tau^{+}体素中不降低，提示NAA水平的降低在Tau蛋白沉积前期及早期阶段更明显，此时Tau蛋白尚未形成广泛NFTs，NAA降低可能与神经炎症和氧化应激反应有关。因此NAA水平降低可作为AD早期诊断的重要生物标志物。Cr是脑内能量代谢标志物，通常用作其他代谢物分析的参考物质[25, 26]。但病理性Tau蛋白位于细胞内，通过影响线粒体功能导致神经元能量代谢障碍，进而引起Cr水平减低[30, 31]。本研究亦发现Tau^{+}体素Cr水平低于HC组和PT组Tau^{-}体素。本研究中PT组和HC组间及各亚组间NAA/Cr水平的差异均无统计学意义，推测可能是因Tau蛋白沉积对Cr水平影响显著，导致AD患者中Cr可能不适合作为其他代谢物分析的参考物质。Cho作为细胞膜磷脂代谢产物，其水平变化反映细胞膜更新状态[25, 26]。既往文献报道，AD患者Cho水平轻度升高或不变[25-28]，其原因并不明朗，可能与神经胶质细胞激活、炎症反应有关[29]，也可能与Tau蛋白沉积存在关联[17, 30, 32]。本研究结果亦显示，PT组和HC组间及各亚组间Cho水平差异均无统计学意义。

PT组Tau^{+}体素中，代谢物水平（含代谢物比值）与Tau PET SUVr的相关性分析显示NAA、Cho、Cr均与SUVr呈负相关。这种负相关性可能反映Tau蛋白沉积对神经元代谢功能的抑制作用[31, 33, 34]。尽管本研究相关性有统计学意义，但相关系数不高，较弱的相关性可能

与以下因素有关。病理因素：AD病理特征具有显著异质性，不同患者Tau蛋白沉积水平和代谢物变化差异较大；除Tau蛋白沉积外，AD病理进程还受其他因素（如淀粉样蛋白沉积、突触密度减低、神经炎症等）影响，这些并存病理可能掩盖Tau蛋白沉积与代谢物水平的直接关联。技术局限性：^{1}H-MRS技术采集范围有限，本研究仅覆盖额顶叶、未包括颞叶、海马等区域。患者因素：AD患者多伴有不同程度脑萎缩，脑萎缩较重、皮层较薄时难以满足体素内2/3的灰质占比，进而影响体素筛选。

综上所述，新型Tau蛋白PET显像剂^{18}F-APN-1607可有效可视化AD患者脑内病理性Tau蛋白沉积。NAA水平降低在Tau蛋白沉积前期及早期更明显，Cr水平改变在Tau蛋白沉积区域更显著，提示NAA及Cr可作为评价AD患者tau蛋白沉积的潜在生物标志物。代谢物水平改变与Tau蛋白沉积的关联机制仍需进一步探索。随着AD疾病修饰治疗的迅速进展，多靶点诊疗指日可待，未来需进一步纵向研究探索脑内病理性蛋白沉积是否伴随其他影像学生物标志物（如^{1}H-MRS检测的代谢物水平）改变，以及这些生物标志物与临床疗效的关联机制。

Declaration of interests: The authors declare no competing interests.

参考文献：

[1] Gin A, Nguyen PD, Serrano G, et al. Towards early diagnosis and screening of Alzheimer's disease using frequency locked whispering gallery mode microtoroid biosensors[J]. Res Sq, 2024: rs. 3. rs-4355995.

[2] Peretti DE, Boccalini C, Ribaldi F, et al. Association of glial fibrillary acid protein, Alzheimer's disease pathology and cognitive decline[J]. Brain, 2024, 147(12): 4094-104.

[3] Jack CliffordJr, , Andrews JS, Beach TG, et al. Revised criteria for diagnosis and staging of Alzheimer's disease: Alzheimer's Association Workgroup[J]. Alzheimers Dement, 2024, 20(8): 5143-69.

[4] Lu JY, Wang J, Wu J, et al. Pilot implementation of the revised criteria for staging of Alzheimer's disease by the Alzheimer's Association Workgroup in a tertiary memory clinic[J]. Alzheimers Dement, 2024, 20(11): 7831-46.

[5] Tahami Monfared AA, Byrnes MJ, White LA, et al. Alzheimer's disease: epidemiology and clinical progression[J]. Neurol Ther, 2022, 11(2): 553-69.

[6] Scheltens P, De Strooper B, Kivipelto M, et al. Alzheimer's disease [J]. Lancet, 2021, 397(10284): 1577-90.

[7] Stelzl LS, Pietrek LM, Holla A, et al. Global structure of the intrinsically disordered protein tau emerges from its local structure [J]. JACS Au, 2022, 2(3): 673-86.

[8] Zhao LH, Teng JL, Mai W, et al. A pilot study on the cutoff value of related brain metabolite in Chinese elderly patients with mild cognitive impairment using MRS[J]. Front Aging Neurosci, 2021, 13: 617611.

[9] Valatkevičienė K, Levin O, Šarkinaitė M, et al. N-acetyl-aspartate and myo-inositol as markers of white matter microstructural organization in mild cognitive impairment: evidence from a DTI-^{1}H-MRS pilot study[J]. Diagnostics (Basel), 2023, 13(4): 654.

[10] Kara F, Joers JM, Deelchand DK, et al. ^{1}H MR spectroscopy biomarkers of neuronal and synaptic function are associated with tau deposition in cognitively unimpaired older adults[J]. Neurobiol Aging, 2022, 112: 16-26.

[11] Li L, Liu FT, Li M, et al. Clinical utility of ^{18}F-APN-1607 tau PET imaging in patients with progressive supranuclear palsy[J]. Mov Disord, 2021, 36(10): 2314-23.

[12] Krix S, Wilczynski E, Falgàs N, et al. Towards early diagnosis of Alzheimer's disease: advances in immune-related blood biomarkers and computational approaches[J]. Front Immunol, 2024, 15: 1343900.

[13] Chang Y, Liu JJ, Xu XD, et al. Subcortical tau deposition and plasma glial fibrillary acidic protein as predictors of cognitive decline in mild cognitive impairment and Alzheimer's disease[J]. Eur J Nucl Med Mol Imaging, 2025, 52(4): 1496-509.

[14] 鲁佳荧, 蒋皆恢, 王 敏, 等. 阿尔茨海默病患者脑内tau蛋白分布与认知组分相关性的PET显像研究[J]. 中国临床神经科学, 2020, 28(4): 396-404.

[15] Qiao Z, Wang GH, Zhao XB, et al. Neuropsychological performance is correlated with tau protein deposition and glucose metabolism in patients with Alzheimer's disease[J]. Front Aging Neurosci, 2022, 14: 841942.

[16] Xu XJ, Ruan WW, Liu F, et al. ^{18}F-APN-1607 tau positron emission tomography imaging for evaluating disease progression in Alzheimer's disease[J]. Front Aging Neurosci, 2022, 13: 789054.

[17] Matthews DC, Kinney JW, Ritter A, et al. Relationships between plasma biomarkers, tau PET, FDG PET, and volumetric MRI in mild to moderate Alzheimer's disease patients[J]. Alzheimers Dement (N Y), 2024, 10(3): e12490.

[18] Ye JW, Wan HL, Chen SH, et al. Targeting tau in Alzheimer's disease: from mechanisms to clinical therapy[J]. Neural Regen Res, 2024, 19(7): 1489-98.

[19] Waheed Z, Choudhary J, Jatala FH, et al. The role of tau proteoforms in health and disease[J]. Mol Neurobiol, 2023, 60(9): 5155-66.

[20] Zhang SM, Crossley CA, Yuan Q. Neuronal vulnerability of the entorhinal cortex to tau pathology in Alzheimer's disease[J]. Br J Biomed Sci, 2024, 81: 13169.

[21] Hu JX, Sha WC, Yuan SS, et al. Aggregation, transmission, and toxicity of the microtubule-associated protein tau: a complex comprehension[J]. Int J Mol Sci, 2023, 24(19): 15023.

[22] Wang M, Wei M, Wang LY, et al. Tau protein accumulation trajectory-based brain age prediction in the Alzheimer's disease continuum[J]. Brain Sci, 2024, 14(6): 575.

[23] Stouffer KM, Chen C, Kulason S, et al. Early amygdala and ERC atrophy linked to 3D reconstruction of rostral neurofibrillary tau tangle pathology in Alzheimer's disease[J]. Neuroimage Clin, 2023, 38: 103374.

[24] Ma D, Fetahu IS, Wang M, et al. The fusiform gyrus exhibits an epigenetic signature for Alzheimer's disease[J]. Clin Epigenetics,

2020, 12(1): 129.

[25] Hu JL, Zhang M, Zhang YY, et al. Neurometabolic topography and associations with cognition in Alzheimer's disease: a whole-brain high-resolution 3D MRSI study[J]. Alzheimers Dement, 2024, 20 (9): 6407-22.

[26] Zhang M, Hu JL, Zhang YY, et al. Associations between Aβ deposition and neurometabolic alterations in Alzheimer's disease: Insights from hybrid 3D MRSI-PET imaging[J]. Alzheimers Dement, 2025, 21(6): e70332.

[27] Sheikh-Bahaei N, Chen M, Pappas I. Magnetic resonance spectroscopy (MRS) in Alzheimer's disease[J]. Methods Mol Biol, 2024, 2785: 115-42.

[28] Kara F, Kantarci K. Understanding proton magnetic resonance spectroscopy neurochemical changes using Alzheimer's disease biofluid, PET, postmortem pathology biomarkers, and APOE genotype[J]. Int J Mol Sci, 2024, 25(18): 10064.

[29] Muñoz-Castro C, Serrano-Pozo A. Astrocyte-neuron interactions in Alzheimer's disease[J]. Adv Neurobiol, 2024, 39: 345-82.

[30] Singh S, Khan S, Shahid M, et al. Targeting tau in Alzheimer's and beyond: insights into pathology and therapeutic strategies[J]. Ageing Res Rev, 2025, 104: 102639.

[31] Olešová D, Dobešová D, Majerová P, et al. Changes in lipid metabolism track with the progression of neurofibrillary pathology in tauopathies[J]. J Neuroinflammation, 2024, 21(1): 78.

[32] Živanović M, Aracki Trenkić A, Milošević V, et al. The role of magnetic resonance imaging in the diagnosis and prognosis of dementia[J]. Biomol Biomed, 2023, 23(2): 209-24.

[33] Abbaspour F, Mohammadi N, Amiri H, et al. Applications of magnetic resonance spectroscopy in diagnosis of neurodegenerative diseases: a systematic review[J]. Heliyon, 2024, 10(9): e30521.

[34] Matsuoka K, Hirata K, Kokubo N, et al. Investigating neural dysfunction with abnormal protein deposition in Alzheimer's disease through magnetic resonance spectroscopic imaging, plasma biomarkers, and positron emission tomography[J]. Neuroimage Clin, 2024, 41: 103560.

（编辑：郎 朗）